



Contents lists available at ScienceDirect

Saudi Journal of Biological Sciences

journal homepage: www.sciencedirect.com

Original article

Statically controlled mycogenic-synthesis of novel biologically active silver-nanoparticles using Hafr Al-Batin desert truffles and its antimicrobial efficacy against pathogens

Shifaa O. Alshammari, Abeer A. Abd El Aty*

Department of Biology, College of Science, University of Hafr Al Batin, P.O. Box 1803, Hafr Al Batin, Saudi Arabia

ARTICLE INFO

Article history:

Received 26 March 2022

Revised 18 April 2022

Accepted 29 May 2022

Available online 1 June 2022

Keywords:

Mycosynthesis

Silver Nanoparticles

Desert Truffle

Response surface methodology (RSM)

Characterization

ABSTRACT

In our search for new unconventional green-reducing agent, can be applied for biosynthesis of biologically active silver-nanoparticles, fruiting bodies (Ascocarps) of Truffle *Terminia* sp. were collected from the sandy desert of Hafr Al-Batin, Eastern Region, Saudi Arabia. The desert truffle showed the ability to reduce AgNO_3 to Ag^0 depending on their high content of proteins (1.74 mg/ml) in the aqueous extract of 30 mg/ml (w/v). The response surface methodology (RSM) with 13 experiments of 2-Factors-5-Level central composite design was applied for controlling all possible combinations of AgNO_3 concentrations and pH values of reaction mixture, which directly affect the particles morphology, size and biological activity. The antimicrobial effectiveness of all synthesized nanoparticles was evaluated against the pathogenic strains by agar diffusion method. The pathogenic Gram-positive *Staphylococcus aureus*, *Bacillus subtilis*, *Lactobacillus cereus*, and Gram-negative *Escherichia coli*, *Salmonella enterica*, yeast strain *Candida albicans* and the fungus *Aspergillus niger* were evaluated. The biologically active Truffle-AgNPs were characterized by UV-visible spectrophotometry, transmission electron microscopy (TEM), spectrum and dynamic light scatter (DLS), and Fourier Transformed Infrared (FTIR). Results obtained indicated that, the statistically controlled Truffle-AgNPs have great inhibitory role affecting different pathogenic strains, which gained much attention towards application of Hafr Al-Batin-Truffle as reducing and stabilizing bio-material for green nano-drugs biosynthesis, to resist harmful pathogens threaten human health.

© 2022 The Author(s). Published by Elsevier B.V. on behalf of King Saud University. This is an open access article under the CC BY-NC-ND license (<http://creativecommons.org/licenses/by-nc-nd/4.0/>).

1. Introduction

Silver-nanoparticles considered one of the most important nanotechnology-derived nanostructures and can be applied in different biomedical fields depending on their promising and interesting properties, as their biological characteristics of antimicrobial activities (Vijayakumara et al., 2019; Ammar et al., 2021). AgNPs showed strong inhibition and assist as a defensive barrier for most of the pathogens, so they are involved in dental

resins, bone adhesive, and medical tools coating (Elechiguerra et al., 2005; Anjum et al., 2016).

Bio-nanotechnology is a new branch of nanotechnology, which integrates principles of biology instead of physical and chemical procedures to generate nano-sized particles with specific functions (Qi and Wang 2004; Roduner 2006; Kathiresan et al. 2009). The bio-based methods for preparation of nanoparticles can be safely scaled up for large scale production as they are simple, relatively inexpensive, economically, and environmentally green (Mohanpuria et al. 2008; Iravani 2011; Prabhu and Poulouse 2012). Biosynthesis of silver-nanoparticles using biological entities such as the extracts of, bacteria, yeast, fungi, algae, or plants attracted researchers in the area of nanotechnology in last few decades (Malik et al. 2014; Alharbi et al., 2020).

Desert truffle (Fagaa) is a fungal species grow naturally in the sand of some deserts after a thunder, lightning storm and heavy rainfall, in Arabian countries found in Middle Eastern region like Libya, Syria, Saudi Arabia, Jordan, and Kuwait (Owaid, 2018). In the Kingdom, the desert of Hafr Al-Batin is rich in truffles especially during the springtime (Manzelat, 2019). The truffles are rich

* Corresponding author.

E-mail addresses: dr.shifaa@uhb.edu.sa (S.O. Alshammari), abeerab@uhb.edu.sa (A.A. Abd El Aty).

Peer review under responsibility of King Saud University.



Production and hosting by Elsevier

in flavonoids (Akyuz, 2013), antioxidants (Murcia et al., 2002), proteins and carbohydrates (Bokhary and Parvez, 1993). Green-synthesis method usually depends on the selection of a bio-reductant, and stabilizer of non-carcinogenic properties for nanoparticles stability (El-Shishtawy et al. 2011). The desert truffle-mediated the synthesis of silver-nanoparticles was preferred over other bio-based preparation methods depending on the reducing activity of the amino acids, by reducing AgNO_3 to Ag^0 (Aldebasi et al., 2014; Khadri et al., 2017).

Response surface methodology (RSM) was an effective technique for controlling the nanoparticles morphology and size, that affecting AgNPs biological activities. In addition, improving the experimental factors like the amount of AgNO_3 , reducing agent, temperature, and pH using central composite design (CCD) decreasing time for rapid AgNPs biosynthesis (Abd El Aty et al., 2020; Ibrahim et al., 2021).

There's no recent data on evaluating the aqueous extract of Hafr Al-Batin truffles, as reducing and capping agent for safe synthesis of biologically active silver-nanoparticles. Therefore, the present study was aimed at synthesis of novel silver-nanoparticles bearing antibacterial and antifungal activities, using the fungal fruit extract of Hafr Al-Batin Desert Truffle *Terminia* sp. An additional aim was to apply a Response Surface Methodology (RSM) of Central Composite Design (CCD) for controlling size and shape of the particles, important for improving the AgNPs antimicrobial activities. All characterizations studies are performed and the antimicrobial importance of Truffle-AgNPs against different pathogenic bacteria, yeast and fungi was investigated.

2. Materials and methods

2.1. Desert truffles samples

Ascocarps (fruiting bodies) of the truffle *Terminia* sp. grown in Hafr Al Batin desert were obtained from a local market in Hafr Al Batin City, Eastern Region, Saudi Arabia. The Fresh Ascocarps were cleaned, sliced, dried at 30–35 °C of the direct sun, until stability of weight, and ground to obtain powder. The truffle powder was kept at room temperature in a dry place until use.

2.2. Extraction of desert truffle Ascocarps

Three grams of dried desert truffle powder, were extracted with 100 ml distilled water by stirring on magnetic stirrer (60 rpm) at 30 °C for sixty min. The crude aqueous extract was centrifuged at 4000 cycle/min for 10 min. and the clear aqueous extract has a concentration of (30 mg/ml) was kept as a stock extract at 2 °C for future studies.

2.3. Evaluation of protein

The desert truffle protein content was determined according to the method of Lowry et al. (1951).

2.4. Bio-synthesis of silver nanoparticles

Five different dilutions of (1.5, 3, 6, 9, 12 mg/ml concentration) were prepared from the truffle-extract stock solution. Ten milliliters of each dilution was mixed with 5 ml of 1 mM AgNO_3 and incubated in 100 rpm rotating shaker at 30 °C for 24 h in a dark place.

2.5. Antimicrobial activity of Truffle-AgNPs

The biosynthesized Truffle-AgNPs (1–5) were screened *in-vitro* against pathogenic strains of gram positive (*Bacillus subtilis* ATCC6633, *Lactobacillus cereus* ATCC14579, *Staphylococcus aureus* ATCC29213), gram negative (*Salmonella enterica* ATCC25566, *Escherichia coli* ATCC25922) bacteria, the yeast (*Candida albicans* ATCC10321) and the fungus (*Aspergillus niger* NRC53) using Agar Well Diffusion (AWD) technique in accordance with Mostafa et al. (2016). Suspensions of all strains were prepared to be approximately (1×10^8 of bacteria and 1×10^6 spores^{-ml} of yeast and fungi). 1 ml of each suspensions was mixed with 50 ml of sterile medium, and poured into a plate. The medium, potato dextrose agar PDA used for yeast and fungi, but nutrient agar medium NA used for bacteria. Wells of about (15 mm in diameter) were made in the solidified-agar-media and filled with 500 μl of AgNPs colloidal solution. The plates were incubated for 24 h at 30–35 °C for bacteria and 72 h at 28–30 °C for yeast and fungi. The average values of inhibition zones IZD were recorded in mm, and reported as Mean \pm SD for three replicates (Abd El Aty and Zohair, 2020).

2.6. Application of Response surface methodology (RSM) for controlled Truffle-AgNPs-antimicrobial activity

For rapid synthesis of AgNPs with controlled size and morphology, the central composite design was applied to control the appropriate concentration of silver nitrate and final pH value of the mixture. The independent variables selected for this study were, A: AgNO_3 (mM) and B: Final pH with different five levels Table 1.

Thirteen experiments of two-factors-five-levels central composite design were carried out to determine the optimal values of (A: AgNO_3) and (B: Final pH). Table 2 showed the matrix of CCD along with nanoparticles antibacterial activity (R1), and antifungal activity (R2), of each trial.

2.6.1. Statistical analysis

The regression and graphical analysis of the data obtained, was evaluated using the Design-Expert[®] 8 software from Stat-Ease. The following quadratic model equation explaining the behavior of the system.

$$Y = \beta_0 + \beta_1A + \beta_2B + \beta_{11}A^2 + \beta_{22}B^2 + \beta_{12}AB.$$

Where Y was the predicted maximum IZD, β_0 ; intercept, β_1 and β_2 ; linear coefficients, β_{11} and β_{22} ; quadratic coefficients and β_{12} ; interactive coefficients. The independent variables A and B were corresponding to AgNO_3 (mM) concentration and final pH respectively. In addition, the statistical analysis of the model was performed to evaluate (ANOVA) analysis that represented as contour plots (3D).

2.7. In-vitro antibacterial and antifungal activity bioassay

Thirteen (1–13) Truffle-AgNPs of central composite design were tested for their antibacterial and antifungal activities using the gram negative bacteria (*Escherichia coli* ATCC25922) and the filamentous fungus (*Aspergillus niger* NRC53). The experiment was applied as mentioned above.

2.8. Characterization studies

2.8.1. UV-visible spectroscopy

Truffle-AgNPs biosynthesis was first detected by color change from pale yellow to reddish brown. the absorption spectrum of the truffle extract was scanned in the range of 200–800 nm on JASCO V-630 UV-VIS Spectrophotometer (JASCO INTERNATIONAL CO., LTD). The sharp characteristic peak at the absorption range of 400–450 nm indicated the preparation of AgNPs.

Table 1
Actual values of tested variables of two-factors-5-levels central composite design (CCD).

| Code | Variable | Range of five levels | | | | |
|------|------------------------|----------------------|------|-----|------|-----------|
| | | $-\alpha$ | -1 | 0 | $+1$ | $+\alpha$ |
| A | AgNO ₃ (mM) | 1.59 | 2 | 3 | 4 | 4.41 |
| B | Final pH | 9.17 | 10 | 12 | 14 | 14.83 |

Table 2
Bioassay of the biosynthesized Truffle-AgNps (1–5) against pathogenic bacteria and fungi.

| Samples (500 µl/ well) | Inhibition zone diameter (IZD) | | | | | | |
|------------------------------|--------------------------------------|---|---|--------------------------------------|--|--------------------------------------|-----------------------------------|
| | Gram-negative bacteria | | Gram-positive bacteria | | | Yeast | Fungi |
| | <i>Escherichia coli</i> ATCC25922 | <i>Salmonella enterica</i> ATCC25566 | <i>Staphylococcus aureus</i> ATCC29213 | <i>Bacillus subtilis</i> ATCC6633 | <i>Lactobacillus cereus</i> ATCC14579 | <i>Candida albicans</i> ATCC10321 | <i>Aspergillus niger</i> NRC53 |
| AgNPs1 | 23 | 18 | 21 | 20 | 19 | 19 | 19 |
| AgNPs2 | 21 | 18 | 20 | 18 | 19 | 18 | 18 |
| AgNPs3 | N.A. | N.A. | N.A. | N.A. | N.A. | N.A. | N.A. |
| AgNPs4 | N.A. | N.A. | N.A. | N.A. | N.A. | N.A. | N.A. |
| AgNPs5 | N.A. | N.A. | N.A. | N.A. | N.A. | N.A. | N.A. |

N.A. no activity.

2.8.2. Transmission electron microscopy (TEM)

Truffle-AgNPs have been characterized by TEM of (JEOL-2100) to evaluate nanoparticles shape and size. The carbon-coated copper grid loaded with AgNps solutions for samples preparation.

2.8.3. Dynamic light scattering analysis (DLS)

Zeta potential and distribution of particle size were measured using Dynamic Light Scattering of two different techniques INTENSITY-Weighted GAUSSIAN DISTRIBUTION Analysis and Zeta-sizer (Particle Sizing Systems, Inc.Santa Barbara, California, USA).

2.8.4. Fourier transforms infrared spectroscopy (FTIR)

For detecting the structural characteristic of main functional groups in the nano-silver solution FTIR spectrometer (JASCO, FT/IR- 6100) was applied in the range of 400–4000 cm⁻¹ at a resolution of 4 cm⁻¹, by employing KBr pellet technique.

3. Results

3.1. Preparation and evaluation of desert Truffle aqueous extract

Fruiting bodies (Ascocarps) of Truffle grown in the sandy desert of Hafr Al-Batin were brought to the laboratory, washed, dried at

room temperature and grounded to obtain powder, used for aqueous extract preparation Fig. 1. Results showed that the prepared stock aqueous extract of (30 mg/ml) (dry w/v) contained high protein concentration of 1.74 mg/ml.

3.2. Biosynthesis of Truffle silver-nanoparticles

For synthesis process of silver nanoparticles, five different dilutions of (1.5, 3.0, 6.0, 9.0 and 12.0 mg/ml) were prepared from the stock extract to determine the best protein concentration preferred for metal reduction and biosynthesis of biologically active AgNPs. Depending on the visual observation, the color of mixture converted from pale yellow to reddish brown with different degree emphasized that all tested concentrations synthesized variable AgNPs (1–5) as shown in Fig. 2.

UV-Visible-Spectra. Fig. 2, declared the successful formation of AgNPs1 obtained from the highest dilution of 1.5 mg/ml, containing about 0.087 mg/ml protein concentration. AgNPs1 showed the maximum absorbance at wavelength 420 nm. Truffle-AgNPs2 prepared with about 0.174 mg/ml protein concentration showed a characteristic peak of 405 nm. On the other hand, three characteristic peaks were observed at 300, 315 and 325 nm respectively, indicated for AgNPs 3, 4 and 5.

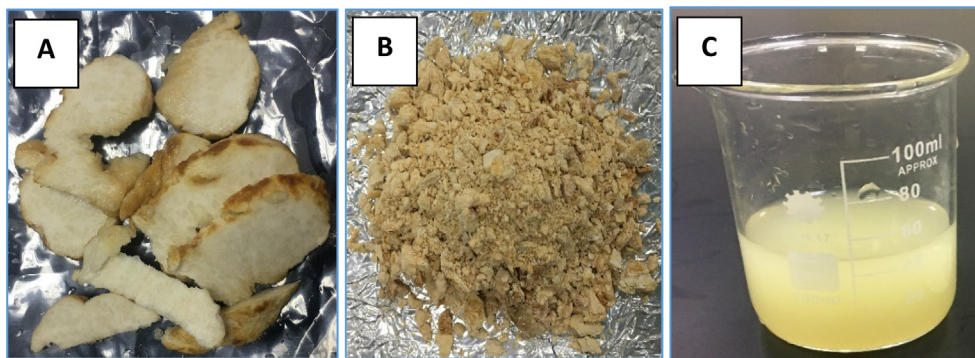


Fig. 1. Desert Truffle (Ascocarps) Slices (A), Dry powder (B), and Aqueous extract (C).

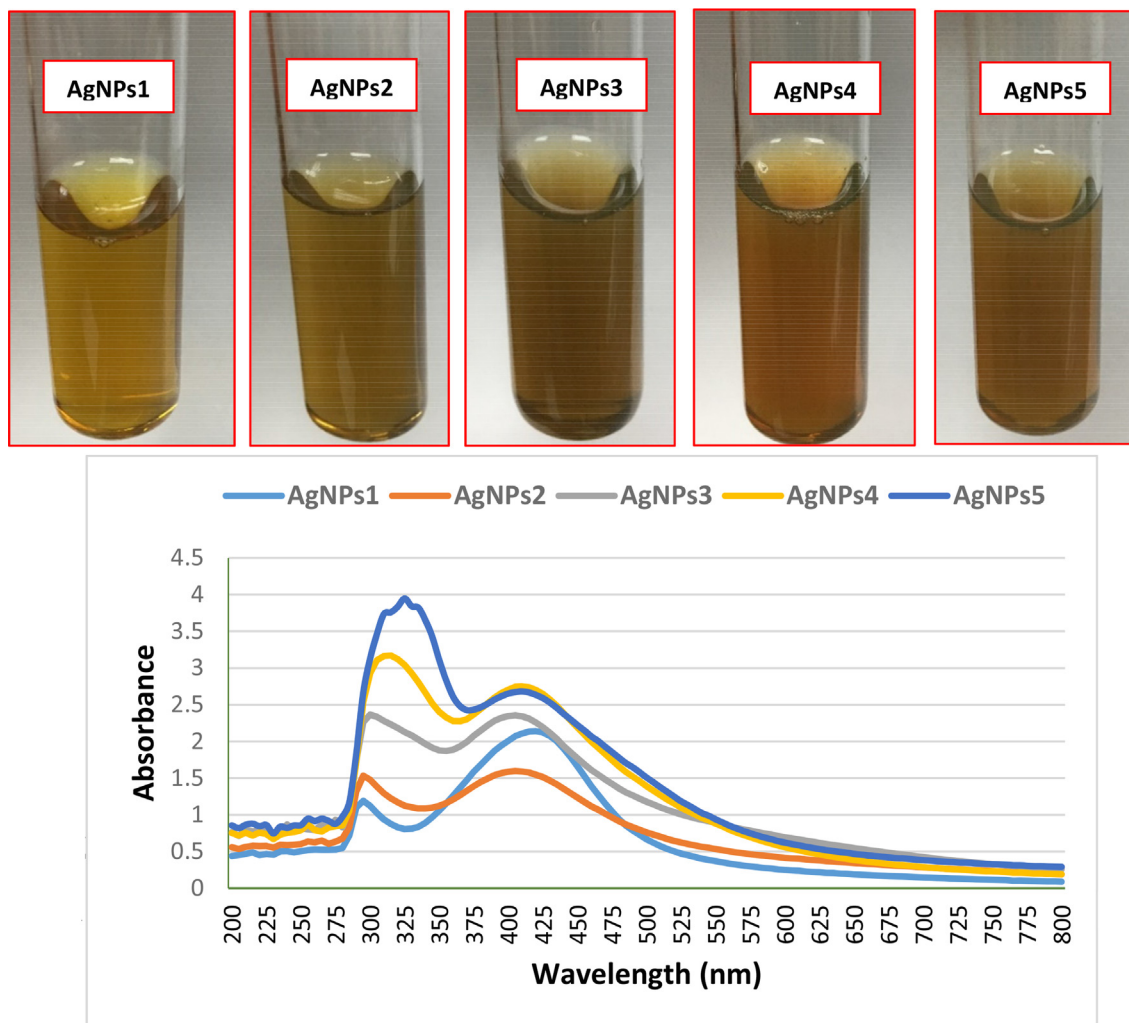


Fig. 2. AgNPs prepared by using five different desert Truffle concentrations after 24 h incubation in dark. UV-Visible spectrum of the synthesized desert Truffle-AgNPs (1–5).

3.3. Antimicrobial activity of biosynthesized Truffle silver-nanoparticles

Bioassay results showed in Table 2 indicated that, AgNPs1 prepared using 0.174 mg/ml protein concentration had the best inhibitory effects, with zones of inhibition in range from (18 to 23 mm) against Gram-negative bacteria, from (19 to 21 mm) against Gram-positive bacteria, and showed 19 mm IZD against the yeast *C. albicans* and filamentous fungus *A. niger*. Truffle-AgNPs2 exhibited a lethal effect towards all gram positive and negative bacterial strains, yeast and fungi, with higher inhibition zone diameter of 21 mm against *E. coli*. However, Truffle-AgNPs 3, 4 and 5 did not exhibit any inhibitory efficacy against tested pathogenic bacterial and fungal strains.

3.4. Application of RSM for improving Truffle silver-nanoparticles antimicrobial activity

Biosynthesis of Truffle-AgNPs was applied in 13 experiments of central composite design (CCD), with all possible combinations of different AgNO_3 concentrations and pH values which are able to change the morphology and size of nanoparticles, which directly affect their biological activity.

All prepared Truffle-AgNPs (1–13) were evaluated against the pathogenic strains *E. coli* and *A. niger* as model examples, for eval-

uation of their antibacterial and antifungal effects. Results obtained in Table 3 indicated that all biosynthesized AgNPs have better antibacterial activities against *E. coli* than the first reaction conditions (1 mM AgNO_3 and pH 7).

Fig. 3 showed the predicted v/s actual values of inhibitory activity against pathogenic tested bacterial R1 and fungal R2 strains. Three dimensional-3D-response surface plots of the two tested variables were showed in Fig. 4. The highest responses 33 and 30 mm-IZD of *E. coli* (R1) were obtained at high AgNO_3 concentration and PH values of the trials number 2, 6 and 11. In addition, AgNPs2, 6 and 11 showed the best antifungal inhibitions of 35, 23 and 35 mm-IZD respectively, against *A. niger* (R2) Fig. 5.

The model accuracy was validated under the maximum conditions, showed the best zones of inhibition (3 mM AgNO_3 , 14.83 pH) for Trail 2, (4 mM AgNO_3 , 14.00 pH) for Trail 6, (2 mM AgNO_3 , 14.00 pH) for Trail 11. Results of Trail 2 showed 33 mm and 35 mm against *E. coli* and *A. niger* respectively were close to the predicted values of 32.12 mm and 34.63 mm. Trail 6 indicated 30 mm and 23 mm, respectively near to the predicted IZD of 31.91 mm and 24.96 mm. Trail 11 showed 30 mm and 35 mm, respectively close to the predicted IZD of 29.91 mm and 34.66 mm.

According to the analysis of variance (ANOVA) of both responses R1 and R2, as shown in (Tables 4 and 5), "Prob > F" < 0.0500 indicated that the quadratic model was significant. Antibacterial activity against *E. coli* (R1) and antifungal activity

Table 3
Factors studied by CCD for controlled Truffle-AgNPs-antimicrobial activity.

| Trial number | Coded levels | | Actual levels | | *R1: IZD of <i>E.Coli</i> (mm) | | *R2: IZD of <i>A. niger</i> (mm) | |
|--------------|--------------------------|------|--------------------------|-------|--------------------------------|-----------|----------------------------------|-----------|
| | A:AgNO ₃ (mM) | B:pH | A:AgNO ₃ (mM) | B:pH | Experimental | Predicted | Experimental | Predicted |
| 1 | 0 | -α | 3.00 | 9.17 | 25 ± 0.17 | 23.88 | 0.00 | 0.00 |
| 2 | 0 | +α | 3.00 | 14.83 | 33 ± 1.02 | 32.12 | 35 ± 0.91 | 34.63 |
| 3 | 0 | 0 | 3.00 | 12.00 | 25 ± 0.19 | 25.00 | 18 ± 0.17 | 18.00 |
| 4 | -1 | -1 | 2.00 | 10.00 | 28 ± 0.00 | 28.09 | 0.00 | 1.79 |
| 5 | 0 | 0 | 3.00 | 12.00 | 25 ± 1.51 | 25.00 | 18 ± 1.04 | 18.00 |
| 6 | +1 | +1 | 4.00 | 14.00 | 30 ± 1.10 | 31.91 | 23 ± 0.18 | 24.96 |
| 7 | +1 | -1 | 4.00 | 10.00 | 20 ± 0.91 | 22.09 | 0.00 | 4.08 |
| 8 | 0 | 0 | 3.00 | 12.00 | 25 ± 1.03 | 25.00 | 18 ± 1.14 | 18.00 |
| 9 | 0 | 0 | 3.00 | 12.00 | 25 ± 0.17 | 25.00 | 18 ± 1.21 | 18.00 |
| 10 | 0 | 0 | 3.00 | 12.00 | 25 ± 0.53 | 25.00 | 18 ± 0.27 | 18.00 |
| 11 | -1 | +1 | 2.00 | 14.00 | 30 ± 1.10 | 29.91 | 35 ± 1.21 | 34.66 |
| 12 | +α | 0 | 4.41 | 12.00 | 29 ± 0.13 | 26.59 | 18 ± 0.21 | 14.50 |
| 13 | -α | 0 | 1.59 | 12.00 | 29 ± 0.19 | 29.41 | 20 ± 1.42 | 19.75 |

*The antibacterial and antifungal effect of AgNPs (1–13) was evaluated by measuring the inhibition zone diameter (IZD) produced around the well in (mm) and the average values of three replicates are reported as Mean ± SD using MS Excel. α = 1.41421.

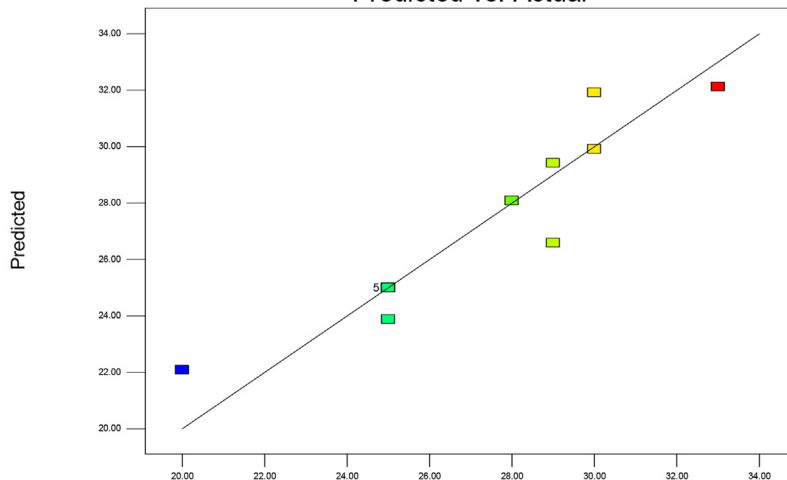
Design-Expert® Software
Antibacterial activity (mm)

Color points by value of
Antibacterial activity (mm):



R1

Predicted vs. Actual



Design-Expert® Software
Antifungal activity (mm)

Color points by value of
Antifungal activity (mm):



R2

Actual
Predicted vs. Actual

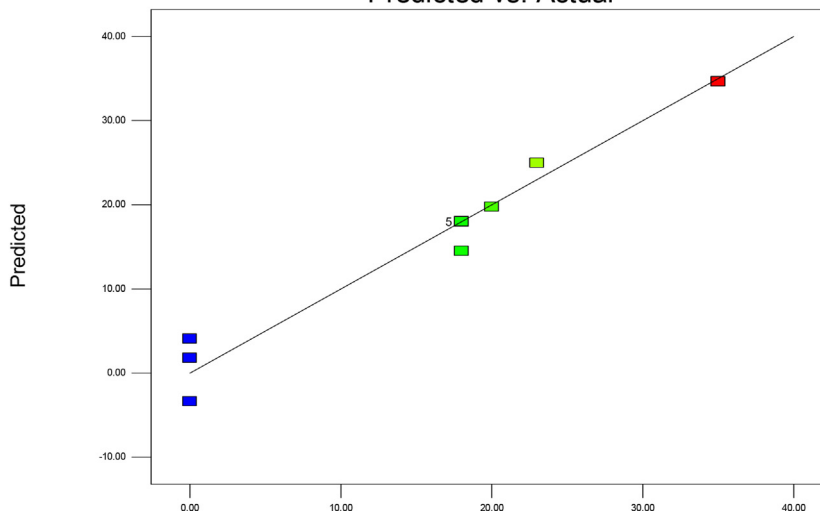


Fig. 3. Distribution of actual (Experimental) and predicted values for Antibacterial (R1), and Antifungal (R2) activities.

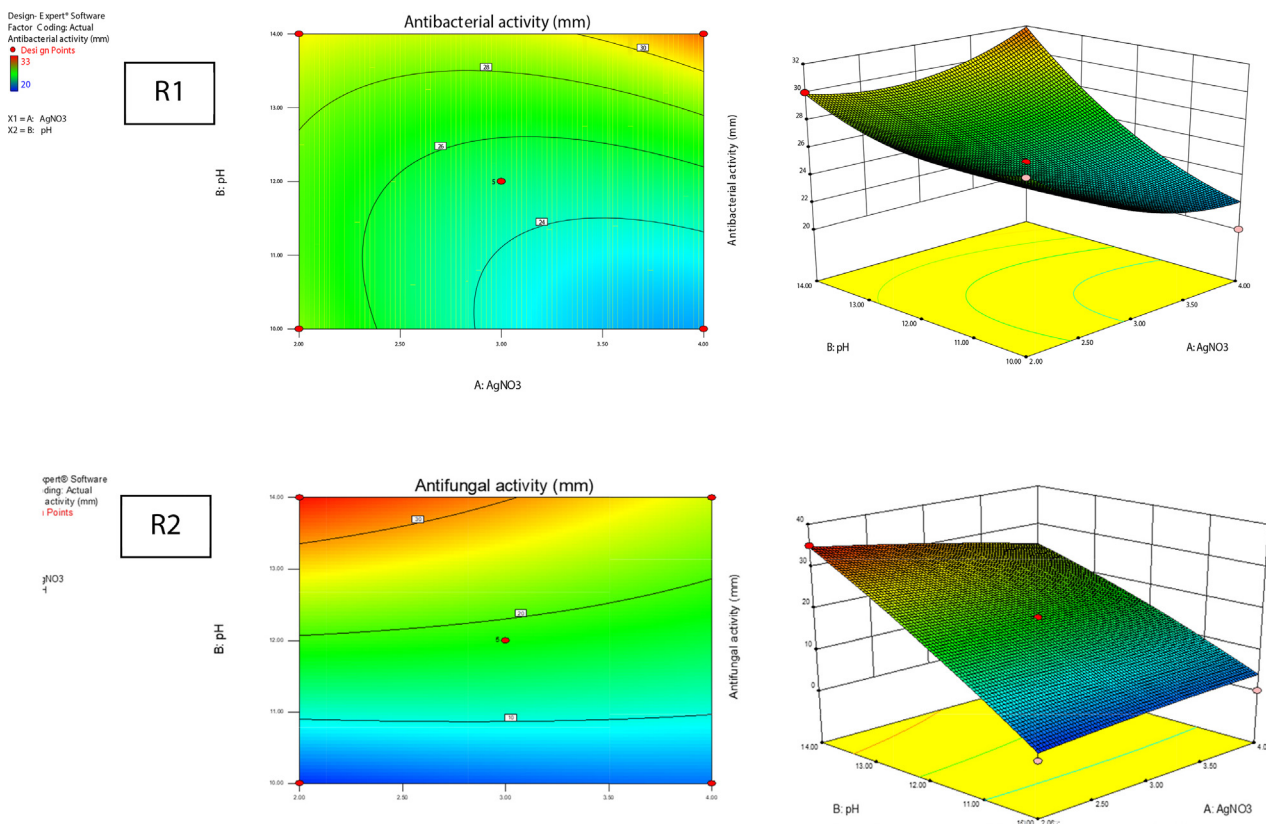


Fig. 4. Response surface plot, showed the effect of AgNO₃ concentrations and pH values on the antibacterial (A) and antifungal (B) activities of Truffle-AgNPs.

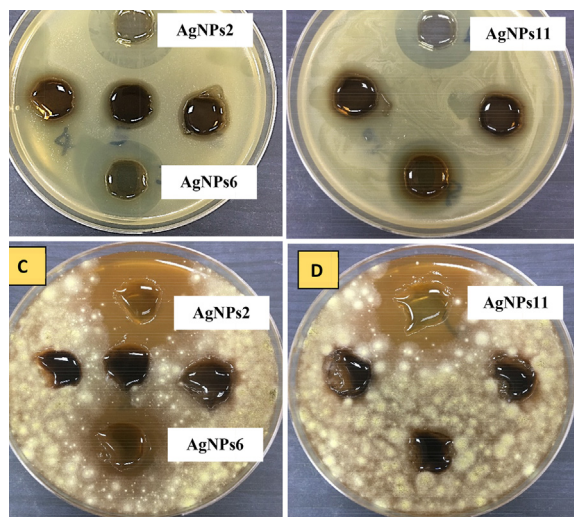


Fig. 5. Antibacterial and antifungal activities of optimized Truffle-AgNPs 2,6 and 11 using (CCD) against *E.coli* (A,B) after 24 h incubation. and *A. niger* (C, D) after 72 h incubation.

against *A. niger* (R2) showed “R-Squared” of 0.8817 and 0.9696 respectively, which advocates for high significance of the model.

The relation between variables and each response was established using a second order polynomial equation in terms of Actual Factors:

$$\text{Antibacterial activity (R1)} = +114.01472 - 22.00000 * \text{AgNO}_3 - 10.54289 * \text{pH} + 1.00000 * \text{AgNO}_3 * \text{pH} + 1.50000 * \text{AgNO}_3^2 + 0.37500 * \text{pH}^2.$$

$$\text{Antifungal activity (R2)} = -157.74995 + 18.77145 * \text{AgNO}_3 + 18.34359 * \text{pH} - 1.50000 * \text{AgNO}_3 * \text{pH} - 0.43750 * \text{AgNO}_3^2 - 0.29688 * \text{pH}^2.$$

According to obtained results the Truffle-AgNPs 2, 6 and 11 were selected out of 13 experiments and characterized.

3.5. Characterization studies

3.5.1. UV-vis spectrum

The prepared samples were measured using UV-visible spectrophotometry. UV-visible absorbance spectra of Truffle-AgNPs2 in range from 200 to 800 nm presented a maximum peak at 415 nm wavelength. Where, Truffle-AgNPs6 and AgNPs11 were clearly observed at 410 nm as seen in Fig. 6.

3.5.2. Transmission electron microscope (TEM)

The potential antimicrobial Truffle-AgNPs 2, 6 and 11 were prepared on a carbon copper grid by dropping a small amount of each sample on the grid and drying it for 5 min. The TEM micrographs was applied at different magnification views of, 200, 100 and 50 nm to show the size and structure of nanoparticles. Images of Truffle-AgNPs 2 and 6 showed that, the majority of nano particles were well stabilized poly-dispersed narrow sizes with spherical shape, and have size range of 7.12 ± 1.17 nm and 8.18 ± 1.52 nm, respectively Fig. 7. Results also showed well-dispersed, cubic to rounded shapes with 11.48 ± 5.72 nm size range of Truffle-AgNPs 11.

To affirm the presence of silver crystal lattice, the area selected electron diffraction (SAED) patterns of Truffle-AgNPs 2, 6 and 11, showed concentric rings with bright spots which reveal that these nanoparticles are highly crystalline in nature in Fig. 7.

Table 4
ANOVA for response surface quadratic model of IZD of *E.coli* (R1).

| Source | Sum of Squares | df | Mean Square | F-value | P-value Prob > F |
|-------------|----------------|----|-------------|---------|---------------------|
| Model | 119.63 | 5 | 23.93 | 10.43 | 0.0038significant |
| A-AgNO3 | 8.00 | 1 | 8.00 | 3.49 | 0.1041 |
| B-pH | 67.94 | 1 | 67.94 | 29.62 | 0.0010 |
| AB | 16.00 | 1 | 16.00 | 6.97 | 0.0334 |
| A2 | 15.65 | 1 | 15.65 | 6.82 | 0.0348 |
| B2 | 15.65 | 1 | 15.65 | 6.82 | 0.0348 |
| Residual | 16.06 | 7 | 2.29 | | |
| Lack of Fit | 16.06 | 3 | 5.35 | | |
| Pure Error | 0.000 | 4 | 0.000 | | |
| Cor Total | 135.69 | 12 | | | |

Std. Dev. 1.51, R-Squared 0.8817, Mean 26.85, C.V. % 5.64, PRESS 114.20, Adeq Precision 9.753.

Table 5
ANOVA for response surface quadratic model of IZD of *A. niger* (R2).

| Source | Sum of Squares | df | Mean Square | F-value | P-value Prob > F |
|-------------|----------------|----|-------------|---------|---------------------|
| Model | 1518.32 | 5 | 303.66 | 44.59 | <0.0001significant |
| A-AgNO3 | 27.49 | 1 | 27.49 | 4.04 | 0.0845 |
| B-pH | 1444.46 | 1 | 1444.46 | 212.08 | < 0.0001 |
| AB | 36.00 | 1 | 36.00 | 5.29 | 0.0551 |
| A2 | 1.43 | 1 | 1.33 | 0.20 | 0.6717 |
| B2 | 8.81 | 1 | 8.81 | 1.44 | 0.2691 |
| Residual | 47.68 | 7 | 6.81 | | |
| Lack of Fit | 47.68 | 3 | 15.89 | | |
| Pure Error | 0.000 | 4 | 0.000 | | |
| Cor Total | 1566.00 | 12 | | | |

Std. Dev. 2.61, R-Squared 0.9696, Mean 17.00, C.V. % 15.35, PRESS 339.03, Adeq Precision 21.457.

3.5.3. Zeta-potential and particle size determination

The biosynthesis of nanoparticles was confirmed by Dynamic Light Scatter analysis (DLS) using two different techniques (INTENSITY-Weighted GAUSSIAN DISTRIBUTION Analysis and Zetasizer). From results obtained, it was detected that, the average size distribution of Truffle-AgNPs 2, 6 and 11, according to INTENSITY-Weighted GAUSSIAN DISTRIBUTION, was found to be 557.9, 242.7, 259.7 nm respectively Fig. 8. And their average zeta-potential, according to Zetasizer analysis, were -6.70, -8.73 and 0.16 mv.

3.5.4. Fourier transforms infrared spectroscopy (FTIR)

The great bio-reductants of desert Truffle extract was identified by FTIR Fig. 9. The FTIR spectrum of all potential AgNPs 2, 6 and 11 was applied. In the current study, the presence of the peak at 3421 cm⁻¹ and 1632 cm⁻¹ are indication for proteins existence. The presence of CN, CS, and CO groups which also indicates the existence of amino acids and proteins were confirmed by peaks of 933 cm⁻¹, 1042 cm⁻¹ and 1079 cm⁻¹. In addition, the peaks at 2527 and 2778 cm⁻¹ indicated the existence of -SH group, and this is another indication for presence of free cysteine or exists at the protein ends.

4. Discussion

The main aim of the present study was to control the green eco-friendly synthesis of novel silver nanoparticles using Truffles grown in desert of Hafr Al-Batin, as reducing and capping bio-agent for safe production and applications in biomedical sectors, as antibacterial and antifungal agent. An additional aim was to apply a Response Surface Methodology (RSM) of Central Composite Design (CCD) for controlling size and shape of the particles, important for improving the AgNPs biological activities.

Black diamond (Truffle) applied in our study is the fruiting body of the ascomycete desert fungus related to the genus *Tuber*, which appeared in the northern region of Saudi Arabia (Khadri et al., 2017; Hussain and Al-Ruqaie, 1999). Truffle were very rich in vitamins A and C, antioxidant, proteins and carbohydrates (Janakat and Nassar, 2010; (Murcia et al., 2002). Depending on the Truffle rich proteins, the amino acids showed reducing activity able to convert AgNO₃ to Ag⁰ as a green process for synthesis of silver nanoparticles, in accordance with Aldebasi et al. (2014). For this purpose, we used Ascocarps (fruiting bodies) of the desert truffle *Terminia* sp. grown in Hafr Al Batin City, Eastern Region, Saudi Arabia. The fruiting bodies were prepared as a stock aqueous extract of (30 mg/ml) (dry w/v) and assayed for protein content according to Lowry et al. (1951), and it appeared contained high protein concentration of 1.74 mg/ml.

The green synthesis of nanoparticles using the desert truffle is more reliable due to the non-toxicity which allows them to be applied in different biomedical fields, when compared to the chemical traditionally methods. Silver nanoparticles were applied in wound dressings, antibacterial applications, cosmetics and drug/gene delivery (Majdalawieh et al., 2014). Depending on the visual observation, the color of mixture converted from pale yellow to reddish brown with different degree emphasized that all tested protein concentrations synthesized numerous AgNPs with variable shapes and sizes. According to Roy et al. (2015) Changing the color of truffle extract is caused by reducing AgNO₃ and discharging of free electrons which form bands of surface plasmon resonance absorption, and the dark color of reaction mixture was stored without change, indicating the nanoparticles stability. Truffle-AgNPs synthesis was confirmed by UV-Visible-Spectra, and the surface plasmon resonance of AgNPs1 indicated at wavelength 420 nm, that's confirm a characteristic plasmon beak for silver nanoparticles formation. Similar findings were observed by Abd El Aty and Ammar (2016) who revealed absorption peak of AgNps at

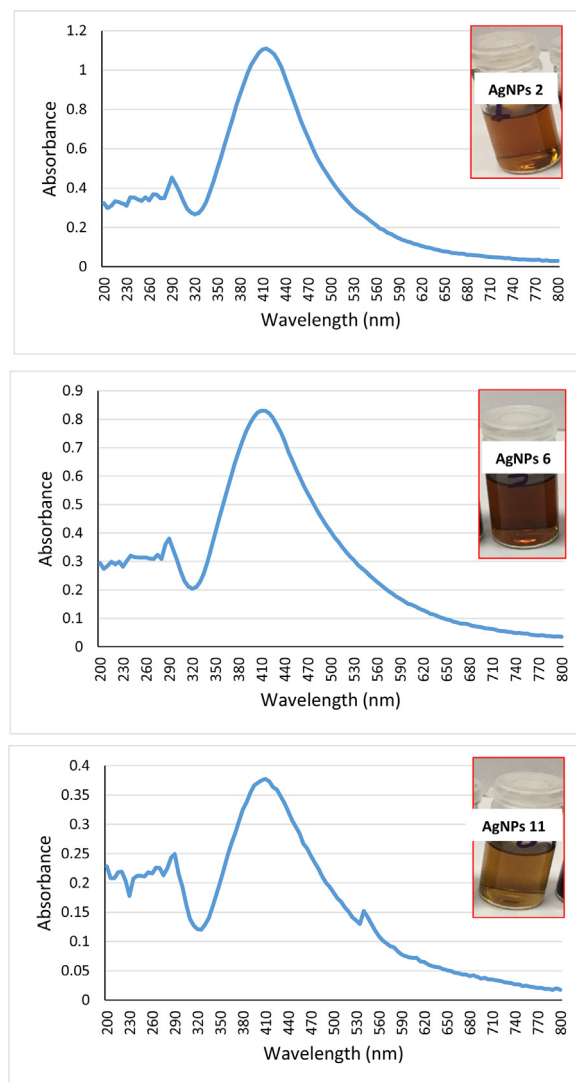


Fig. 6. UV-Vis spectra analysis of biosynthesized Truffle-AgNPs 2, 6 and 11.

430 nm using marine-derived fungus *Alternaria tenuissima* KM651985. In addition, silver nanoparticles derived from *Terfezia clavertyi* was clearly observed at 440 nm (Khadri et al., 2017). Truffle-AgNPs2 showed a characteristic peak of 405 nm which also confirmed the formation of nano-silver. But the peaks appeared at 300, 315 and 325 nm respectively for AgNPs 3, 4 and 5, refer to the presence of unreduced metal and formation of particles with larger sizes, therefore aggregates might be found in these samples. This phenomenon indicated that the protein of 0.348, 0.522 and 0.696 mg/ml concentrations not favorable for reducing 1 mM AgNO_3 to Ag^0 , with low capping ability (Ammar et al., 2021).

All biosynthesized Truffle-AgNPs (1–5) were biologically evaluated for their antibacterial and antifungal activities according to (Shahen and Abd El Aty, 2018). Antimicrobial bioassay indicated the good inhibitory effects of Truffle-AgNPs1 and AgNPs2 against all tested pathogenic bacteria and fungi, but Truffle-AgNPs 3, 4 and 5 did not exhibit any inhibitory efficacy against tested pathogenic strains. This good antibacterial activity is mainly because, nano silver with small size in range of 8.46 ± 5.13 nm stick to the sulfur-containing proteins of the bacterial cell membrane. At

the membrane a silver-sulfur-interaction takes place, which directly causes many morphological and structural changes in the bacterial cell wall, leading to the release out of the cellular components (Feng et al., 2000). Also nanoparticles may move to the inside of bacterial cell causing nucleic acid interaction, which directly inhibited the proteins replication and lead to the death of microbial cells (Klasen, 2000).

The toxicity effects of AgNPs usually depends on different great factors such as reducing agent source, particles size and morphology, stability rate of nano particles, charges of particles and the type of pathogenic organisms (Azam et al., 2012). Therefore, the Response surface methodology (RSM) with 13 experiments was applied for controlling the nanoparticles morphology and size, and help rapid AgNPs biosynthesis. (Abd El Aty et al., 2020; Ibrahim et al., 2021). All prepared Truffle-AgNPs (1–13) have better antimicrobial activities than the first reaction conditions (1 mM AgNO_3 and pH 7). Statistical analysis of the design indicated a suitable fit and satisfactory correlation of obtained (actual) and predicted values as shown by the closer clusters to the diagonal line in the parity plot. AgNPs of trials number 2, 6 and 11 showed the highest antibacterial and antifungal responses, with the reaction conditions of high AgNO_3 concentration and PH values of. Other results were discussed by Owaid et al. (2018) who reported the zone of inhibition 11 and 9.5 mm by applying 10 mg-truffle-AgNPs against *Escherichia coli* and *Klebsiella spp.*. The results obtained by Muhsin and Hachim (2016) showed that *Tirmania nivea* silver-nanoparticles exhibited an inhibition activity of (14.5–28 mm inhibition zones diameter) against the tested pathogenic bacterial strains like *E. coli* and *P. aeruginosa*. The model accuracy was validated under the maximum conditions, showed the best IZDs of trials 2, 6 and 11 and the obtained data showed the efficiency of the applied model and indicated the dependence of particles activity on the reaction conditions which affected the particles size and shape (Abd El Aty et al., 2020).

Analysis of variance (ANOVA) showed “R-Squared” of 0.8817 and 0.9696 of responses 1 and 2 respectively, which advocates for high significance of the model, and obtained results indicated that the design of 2-factors-5-levels (CCD) was very applicable for biosynthesis of high biologically active Truffle-AgNPs under controlled conditions of AgNO_3 concentration and pH value. Therefore, Truffle-AgNPs 2, 6 and 11 were selected and characterized. Truffle-AgNPs were first, characterized by changing the mixture color from pale yellow to dark brown after 24 h of incubation in a dark place according to Owaid (2022). Second, the UV-visible spectrophotometry of Truffle-AgNPs samples presented a maximum peak at 415 nm and 410 nm. All obtained sharp peaks given by UV visible spectrum at the absorption range 400–450 nm has indicated the formation of AgNPs according to Shaheen & Abd El Aty (2018). Different magnification views of TEM micrographs was applied at, 200, 100 and 50 nm to show the size and structure of nanoparticles. The majority of Truffle-AgNPs 2 and 6 particles were well stabilized poly-dispersed narrow sizes with spherical shape, and have size range of 7.12 ± 1.17 nm and 8.18 ± 1.52 nm, respectively, on the other hand Truffle-AgNPs 11 particles were well-dispersed, cubic to rounded with a size range of 11.48 ± 5.72 nm. Other studies of Owaid (2022) showed AgNPs with average size of 72 nm with irregular to spherical shapes, synthesized from desert truffle grown in Anbar desert, Iraq. Khadri et al. (2017) shown that *T. clavertyi*-AgNPs were spherical shape with large sizes ranging between 40 and 60 nm, but Muhsin and Hachim (2016) showed *Tirmania nivea*-AgNPs with sizes ranging from 3 nm to 41 nm with dispersed spherical shapes. According to INTENSITY-Weighted GAUSSIAN DISTRIBUTION, Truffle-AgNPs 2, 6 and 11 was found to be 557.9, 242.7,

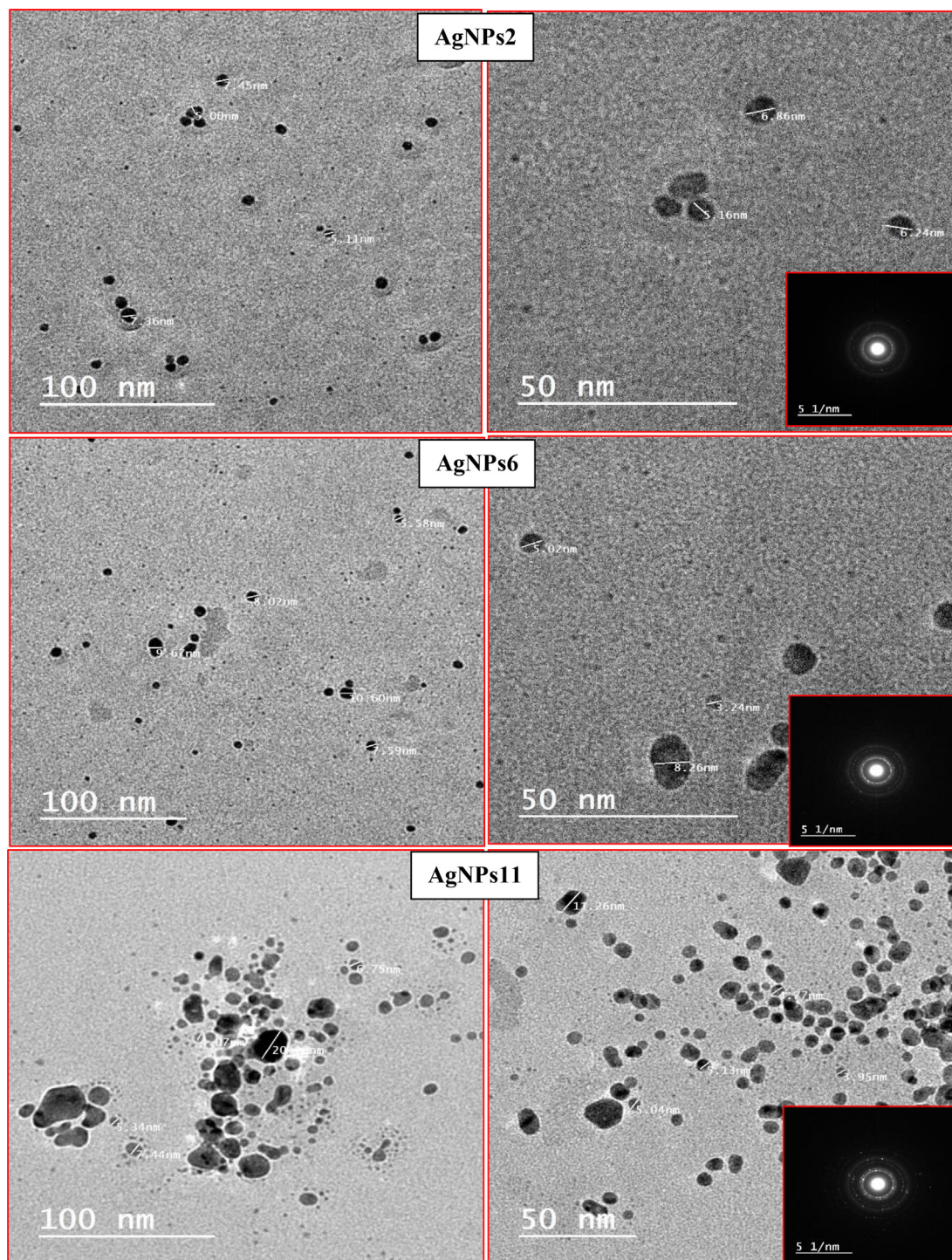


Fig. 7. TEM micrographs of the potential antimicrobial Truffle-AgNPs 2, 6 and 11. Inset shows selected area electron diffraction (SAED) patterns of nanoparticles.

259.7 nm respectively, and their average zeta-potential, according to Zetasizer analysis, were -6.70 , -8.73 and 0.16 mv, the negative charge refers to physical stability of AgNPs. Abd El Aty and Moustafa (2020) observed a characteristic peak of AgNPs with average size of 119.8 nm using zeta sizer, and Ammar et al., (2021) obtained AgNPs with Zeta potential of -32.8 and -45.9 . FTIR spectrum of AgNPs2, 6 and 11 peaks showed peaks at 3421 cm^{-1} and 1632 cm^{-1} indicating proteins existence. The presence of CN,

CS, and CO groups which indicates the existence of amino acids and proteins were confirmed by peaks of 933 cm^{-1} , 1042 cm^{-1} and 1079 cm^{-1} . In addition, the peaks at 2527 and 2778 cm^{-1} indicated the existence of $-SH$ group, and this is another indication for presence of free cysteine or exists at the protein ends. Silverstein et al., (2005) showed similar results. The recorded results of FTIR analysis confirmed the presence of proteins which can be served as capping and reducing agents.

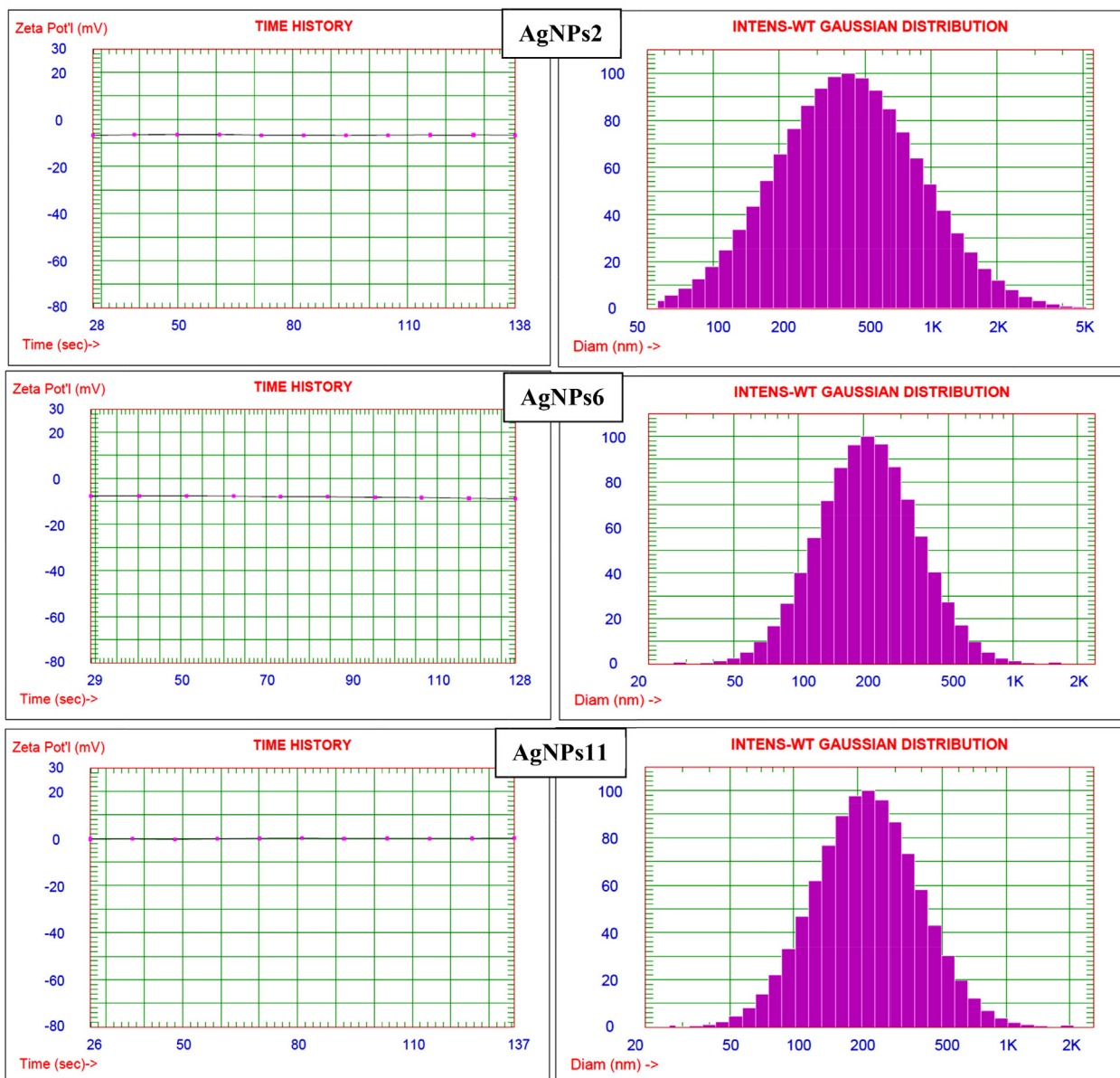


Fig. 8. Dynamic light-scattering analysis (DLS) of Truffle-AgNPs 2, 6 and 11.

5. Conclusion

The current study reveals the potential application of Truffle-fruited bodies (*Ascocarps*) as green-reducing and capping agent for biosynthesis of silver-nanoparticles. Truffle aqueous extract of 1.5 mg/ml (w/v), showed the best protein concentration 0.087 mg/ml preferred for biosynthesis of antimicrobial AgNPs. RSM of 2-factors-5-levels (CCD) was very applicable for biosynthesis of high biologically active Truffle-AgNPs under controlled

conditions of $AgNO_3$ concentration and pH value. Results revealed the best trails number 2,6 and 11 for biosynthesis of antimicrobial AgNPs with polydispersed particle size ranged 7.12, 8.18 and 11.48 nm respectively as indicated from TEM micrographs. Moreover, UV-visible spectrophotometry, DLS and FTIR investigations confirmed the formation of Truffle-AgNPs. Finally, mycosynthesized Truffle-AgNPs exhibited good inhibitory effects against harmful pathogenic bacteria and fungi.

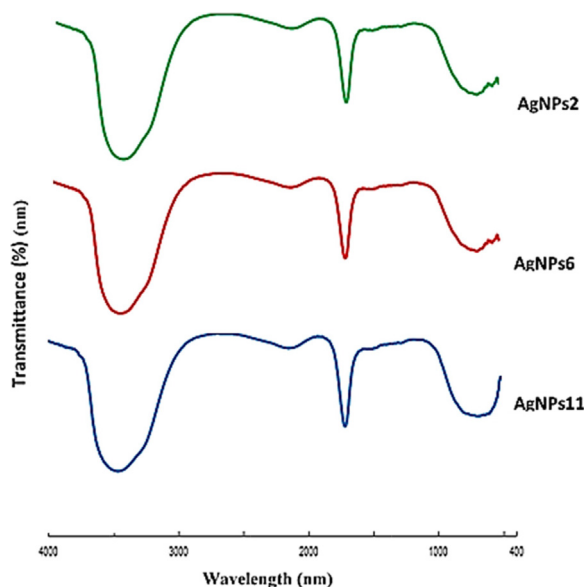


Fig. 9. FTIR spectrum of of Truffle-AgNPs 2, 6 and 11.

Funding

This study was supported by the Deanship of Scientific Research, University of Hafr Al Batin project No (0006-1443-S).

Declaration of Competing Interest

The authors declare that they have no known competing financial interests or personal relationships that could have appeared to influence the work reported in this paper.

Acknowledgement

The authors extend their appreciation to the Deanship of Scientific Research, University of Hafr Al Batin for funding this work through the research group project No (0006-1443-S).

Appendix A. Supplementary data

Supplementary data to this article can be found online at <https://doi.org/10.1016/j.sjbs.2022.103334>.

References

- Abd El Aty, A.A., Ammar, H.A., 2016. Potential characterization and antimicrobial applications of newly bio-synthesized silver and copper nanoparticles using the novel marine-derived fungus *Alternaria tenuissima* KM651985. *Research Journal of BioTechnology* 11 (8), 71–82.
- Abd El Aty, A.A., Zohair, M.M., 2020. Green-synthesis and optimization of an eco-friendly nanobiofungicide from *Bacillus amyloliquefaciens* MH046937 with antimicrobial potential against phytopathogens. *Environ. Nanotechnol. Monit. Manage.* 14, <https://doi.org/10.1016/j.enmm.2020.100309>.
- Abd El Aty, A.A., Mohamed, A.A., Zohair, M.M., Soliman, A.A.F., 2020. Statistically controlled biogenesis of silver nano-size by *Penicillium chrysogenum* MF318506 for biomedical application. *Biocatal. Agric. Biotechnol.* 25, 101592. <https://doi.org/10.1016/j.bcab.2020.101592>.
- Akyuz, M., 2013. Nutritive value, flavonoid content and radical scavenging activity of the truffle (*Terfezia boudieri* Chatin). *J. Soil Sci. Plant Nutr.* 13 (1), 143–151.
- Aldebasi, Y.H., Aly, S.M., Riazunnisa, K., Khadri, H., 2014. Noble silver nanoparticles (AgNPs) synthesis and characterization of fig-leaf (*Ficus carica*) extract and its antimicrobial effect against clinical isolates from corneal ulcer. *Afr. J. Biotechnol.* 13 (45), 4275–4281.

- Alharbi, R.M., Soliman, A.A.F., Abd El Aty, A.A., 2020. Comparative study on biosynthesis of valuable antimicrobial and antitumor nano-silver using fresh water green and blue-green microalgae. *J. Microbiol. Biotechnol. Food Sci.* 10 (2), 2020 <https://www.jmbfs.org/wp-content/uploads/2020/10/1852-Main-document-manuscript-preprint.pdf>.
- Ammar, H.A., Abd El Aty, A.A., El Awdan, S.A., 2021. Extracellular myco-synthesis of nano-silver using the fermentable yeasts *Pichia kudriavzevii*HA-NY2 and *Saccharomyces uvarum*HA-NY3, and their effective biomedical applications. *Bioprocess Biosyst. Eng.* 44 (4), 841–854. <https://doi.org/10.1007/s00449-020-02494-3>.
- Anjum, S., Abbasi, B.H., Shinwari, Z.K., 2016. Plant-mediated green synthesis of silver nanoparticles for biomedical applications: Challenges and opportunities. *Pak. J. Bot.* 48, 1731–1760.
- Azam, A., Ahmed, A.S., Oves, M., Khan, M.S., Memic, A., 2012. Sizedependent antimicrobial properties of CuO nanoparticles against Gram-positive and -negative bacterial strains. *Int. J. Nanomed.* 7, 3527–3535.
- Bokhary, H.A., Parvez, S., 1993. Chemical composition of desert truffles *Terfezia clavaryi*. *J. Food Comp. Anal.* 6 (3), 285–293.
- Elechiguerra, J.L., Burt, J.L., Morones, J.R., Camacho-Bragado, A., Gao, X., Lara, H.H., Yacaman, M.J., 2005. Interaction of silver nanoparticles with HIV-1. *J. Nanobiotechnol.* 29, 3–6. <https://doi.org/10.1186/1477-3155-3-6>.
- El-Shishtawy, R.M., Asiri, A.M., Al-Otaibi, M.M., 2011. Synthesis and spectroscopic studies of stable aqueous dispersion of silver nanoparticles. *Spectrochim. Acta Part A Mol. Biomol. Spectrosc.* 79 (5), 1505–1510. <https://doi.org/10.1016/j.saa.2011.05.007>.
- Feng, Q.L., Wu, J., Chen, G.Q., Cui, F.Z., Kim, T.N., Kim, J.O., 2000. A mechanistic study of the antibacterial effect of silver ions on *Escherichia coli* and *Staphylococcus aureus*. *J. Biomed. Mater. Res.* 52 (4), 662–668.
- Hussain, G., Al-Ruqaie, I.M., 1999. Occurrence, chemical composition, and nutritional value of truffles: an overview. *Pak. J. Biol. Sci.* 2 (2), 510–514.
- Ibrahim, S., Ahmad, Z., Manzoor, M.Z., Mujahid, M., Faheem, Z., Adnan, A., 2021. Optimization for biogenic microbial synthesis of silver nanoparticles through response surface methodology, characterization, their antimicrobial, antioxidant, and catalytic potential. *Sci. Rep.* 11, 770. <https://doi.org/10.1038/s41598-020-80805-0>.
- Iravani, S., 2011. Green synthesis of metal nanoparticles using plants. *Green Chem.* 13 (10), 2638–2650. <https://doi.org/10.1039/C1GC15386B>.
- Janakat, S., Nassar, M., 2010. Hepatoprotective activity of desert truffle (*Terfezia clavaryi*) in comparison with the effect of *Nigella sativa* in the rat. *Pak. J. Nutr.* 9 (1), 52–56.
- Kathiresan, K., Manivannan, S., Nabeel, M.A., Dhivya, B., 2009. Studies on silver nanoparticles synthesized by a marine fungus, *Penicillium fellutanum* isolated from coastal mangrove sediment. *Colloids Surf. B* 71 (1), 133–137. <https://doi.org/10.1016/j.colsurfb.2009.01.016>.
- Khadri, H., Aldebasi, Y.H., Riazunnisa, K., 2017. Truffle mediated (*Terfezia clavaryi*) synthesis of silver nanoparticles and its potential cytotoxicity in human breast cancer cells (MCF-7). *Afr. J. Biotechnol.* 16 (22), 1278–1284. <https://doi.org/10.5897/AJB2017.16031>.
- Klasen, H.J., 2000. A historical review of the use of silver in the treatment of burns. *Burns* 26 (2), 117–130.
- Lowry, O.H., Rosebrough, N.J., Farr, A.L., Randall, R.J., 1951. Protein measurement with folin phenol reagent. *J.B.C.* 193, 265–275.
- Majdalawieh, A., Kanan, M.C., El-Kadri, O., Kanan, S.M., 2014. Recent advances in gold and silver nanoparticles: synthesis and applications. *J. Nanosci. Nanotechnol.* 14 (7), 4757–4780.
- Malik, P., Shankar, R., Malik, V., Sharma, N., Mukherjee, T.K., 2014. Green chemistry based benign routes for nanoparticle synthesis. *J. Nanopar.* 2014, 1–14. <https://doi.org/10.1155/2014/302429>.
- Manzelat, S.M., 2019. Mushrooms in Saudi Arabia (local and imported). *Int. J. Curr. Res. Biosci. Plant Biol.* 6 (8), 8–12. <https://doi.org/10.20546/ijcrbp.2019.608.002>.
- Mohanpuria, P., Rana, N., Yadav, S., 2008. Biosynthesis of nanoparticles: technological concepts and future applications. *J. Nanopart. Res.* 10 (3), 507–517. <https://doi.org/10.1007/s11051-007-9275-x>.
- Mostafa, F.A., Abd El Aty, A.A., Hamed, E.R., Eid, B.M., Ibrahim, N.A., 2016. Enzymatic, kinetic and anti-microbial studies on *Aspergillus terreus* culture filtrate and *Allium cepa* seeds extract and their potent applications. *Biocatal. Agric. Biotechnol.* 5, 116–122.
- Muhsin, T.M., Hachim, A.K., 2016. Characterization and Antibacterial Efficacy of Mycosynthesized Silver Nanoparticles from the Desert Truffle *Tirmania nivea*. In: Qatar Foundation Annual Research Conference Proceedings. HBPP1149. <https://doi.org/10.5339/qfarc.2016.HBPP1149>.
- Murcia, M.A., Martínez-Tomé, M., Jiménez, A.M., Vera, A.M., Honrubia, M., Parras, P., 2002. Antioxidant activity of edible fungi (Truffles and Mushrooms): Losses during industrial processing. *J. Food Prot.* 10 (9), 1614–1622.
- Owaid, M.N., 2022. Biosynthesis of Silver Nanoparticles from Truffles and Mushrooms and Their Applications as Nanodrugs. *Curr. Appl. Sci. Technol.* 22 (5), 1–11. <https://doi.org/10.55003/cast.2022.05.22.009>.
- Owaid, M.N., Muslim, R.F., Hamad, H.A., 2018. Mycosynthesis of Silver Nanoparticles using *Terminia* sp. Desert Truffle, Pezizaceae, and their Antibacterial Activity. *Jordan J. Biol. Sci.* 11 (4), 401–405.
- Prabhu, S., Poulouse, E., 2012. Silver nanoparticles: mechanism of antimicrobial action, synthesis, medical applications, and toxicity effects. *Int. Nano Lett.* 2 (1), 1–10. <https://doi.org/10.1186/2228-5326-2-32>.

- Qi, W.H., Wang, M.P., 2004. Size and shape dependent melting temperature of metallic nanoparticles. *Mater. Chem. Phys.* 88, 280–284. <https://doi.org/10.1016/j.matchemphys.2004.04.026>.
- Roduner, E., 2006. Size matters: why nanomaterials are different. *Chem. Soc. Rev.* 35 (7), 583–592. <https://doi.org/10.1039/B502142C>.
- Roy, K., Sarkar, C.K., Ghosh, C.K., 2015. Photocatalytic activity of biogenic silver nanoparticles synthesized using yeast (*Saccharomyces cerevisiae*) extract. *Appl. Nanosci.* 5 (8), 953–959.
- Shaheen, T.I., Abd El Aty, A.A., 2018. In-situ green myco-synthesis of silver nanoparticles onto cotton fabrics for broad spectrum antimicrobial activity. *Int. J. Biol. Macromol.* 118, 2121–2130.
- Silverstein, R., Webster, F., Kiemle, D., 2005. *Spectrometric Identification of Organic Compounds*. John Wiley and Sons Inc, pp. 72–126.
- Vijayakumara, S., Malaikozhundana, B., Saravanakumar, K., Duran-Larac, E.F., Wang, M., Vaseeharana, B., 2019. Garlic clove extract assisted silver nanoparticle—antibacterial, antibiofilm, antihelminthic, anti-inflammatory, anticancer and ecotoxicity assessment. *J. Photochem. Photobiol. B* 198, 111558. <https://doi.org/10.1016/j.jphotobiol.2019.111558>.